Splitting the surface wave in metal/dielectric nanostructures

Zhu Song(祝 颂)† and Wu Jian(吴 坚)

Department of Physics, State Key Laboratory of Advanced Optical Communication Systems and Networks, Shanghai Jiao Tong University, Shanghai 200240, *China*

(Received 3 September 2010; revised manuscript received 17 November 2010)

We investigate a modified surface wave splitter with a double-layer structure, which consists of symmetrical metallic grating and an asymmetrical dielectric, using the finite-difference time-domain (FDTD) simulation method. The metal/dielectric interface structure at this two-side aperture can support bound waves of different wavelengths, thus guiding waves in opposite directions. The covered dielectric films play an important role in the enhancement and confinement of the diffraction wave by the waveguide modes. The simulation result shows that the optical intensities of the guided surface wave at wavelengths of 760-nm and 1000-nm are about 100 times and 4∼5 times those of the weaker side, respectively, which means that the surface wave is split by the proposed device.

Keywords: surface plasmons, finite-difference time-domain method, metallic grating, layered nanostructures

PACS: 79.60.Jv, 91.30.Fn, 02.60.Cb **DOI:** 10.1088/1674-1056/20/6/067901

1. Introduction

The optical properties of metallic nanostructures have aroused great interest in both theory and experiment since the extraordinary optical transmission through two-dimensional sub-wavelength periodic hole arrays milled on a thin metal film discovered by Ebbessen *et al.*[1] Metallic photonic materials demonstrate unique properties due to the existence of metals on electromagnetic surface waves known as surface plasmons (SPs). SPs open up possibilities for photonics because they allow the concentration and propagation of light below their usual resolution limits, thus opening up possibilities for subwavelength optical components. The optical properties of plasmonic structures and devices have been investigated in various cases.[2−4] Recently, a metal film with a single aperture surrounded by metallic grating in the input surface (on which the incident light impinges) or output surface drew a lot of attention for its good performance in enhancing transmission and light beaming.[5−10] The focal length of the beaming light is determined by the geometrical parameters of the output surface.[11,12] Martin-Moreno *et al.*[13] found that the angular distribution of the diffracted light can be changed by tuning the geometrical parameters of the grooves. In addition, in some cases the transmission light is confined in an output surface rather than being coupled to a far field if the parameters of grooves satisfy a certain relation. Further, structures with different surface structures located on the two sides of the slit, which can split waves of different wavelengths, were designed.[14,15]

In this paper, we propose a surface wave splitter with symmetrical output surface metallic grating covered by an asymmetrical dielectric slab, which can guide surface waves of different wavelengths towards opposite directions. We use different refractive indices to achieve the surface wave splitting rather than different grating geometrical parameters.

2. Theoretical framework and simulation setup

SPs are a special kind of electromagnetic field, which can propagate along the interface between a metal and a dielectric medium while keeping bounded near the surface without radiating away.[16] The SP mode is excited on the surface when a p-polarized wave (the magnetic field is perpendicular and the electric field is parallel to the propagating two-dimensional plane) impinges on a metallic film. Solving Maxwell's equations under the appropriate bound-

†Corresponding author. E-mail: songzhu85@gmail.com

© 2011 Chinese Physical Society and IOP Publishing Ltd

ary conditions yields the SP dispersion relation[17]

$$\boldsymbol{k}_{\rm sp} = \boldsymbol{k}_0 \sqrt{\frac{\varepsilon_{\rm m}\varepsilon_{\rm d}}{\varepsilon_{\rm m}+\varepsilon_{\rm d}}}, \tag{1}$$

where $\boldsymbol{k}_{\rm sp}$ represents the SP wave vector and $\boldsymbol{k}_0$ is the wave vector in free space. The frequency-dependent permittivity of the metal $\varepsilon_{\rm m}$ and the dielectric material $\varepsilon_{\rm d}$ must have opposite signs for SPs to be possible at such an interface. This condition is satisfied for metals because $\varepsilon_{\rm m}$ is both negative and complex. The interaction between the surface charge density and the electromagnetic field leads the momentum of the SP mode wave vector to be greater than that of a free-space photon of the same frequency. This increase in momentum is associated with the binding of the SP to the surface, and the resulting momentum mismatch between light and SPs of the same frequency must be bridged if light is to be used to generate SPs. It implies that light cannot convert to SPs directly on a flat surface. One way to couple the free propagating light with SPs is to produce a patterned structure that is periodic on the scale of the wavelength.[18] More importantly, the process can be reversed. It allows the otherwise non-radiative SP mode to couple with light in an efficient and controlled way.[19,20] It is well known that the grooves on the input surface can enhance the near field intensity[21] and is not very related to the output surface wave distribution; the distribution of the transmitted light depends only on the structure of the output surface. In this proposed device, the input surface grooves do not have a direct connection with the output surface grooves. The light splitting phenomenon still occurs when the incident surface is flat, although the transmitted optical intensity is weaker. Therefore, we investigate the output properties of light only through adjusting the corrugated output metal/dielectric interface.

Figure 1(a) shows the schematic diagram of the proposed device structure. The thickness of the silver film is $H_{\rm m}$ with a single 100-nm width slit surrounded by $2M$ grooves on the input surface and $2N$ grooves on the output surface. These grooves on the input and the output surfaces are periodically distributed and symmetrically located with respect to the central slit. The period of the input surface structure is $P_{\rm b}$, the width of each groove is $W_{\rm b}$ and the height is $H_{\rm b}$. The grooves on the output surface have the period $P_{\rm a}$, width $W_{\rm a}$ and height $H_{\rm a}$. The thickness of the two dielectric layers covered on both sides of the metal film is $H_{\rm d}$. The permittivity of the dielectric film on the left/right side of the slit is n_1/n_2, respectively. All of the parameter symbols are labeled in Fig. 1, their values are given as follows: the width of the slit is 100 nm; $M = 8$, $N = 11$; $P_{\rm b} = 600$ nm, $W_{\rm b} = 300$ nm, $H_{\rm b} = 100$ nm; $P_{\rm a} = 400$ nm, $W_{\rm a} = 200$ nm, $H_{\rm a} = 80$ nm; $H_{\rm m} = 800$ nm, $H_{\rm d} = 300$ nm; $n_1 = 1.52$, $n_2 = 2$. We set the centre of the slit at the input metal surface as the origin of the coordinate ($x = 0$, $z = 0$).

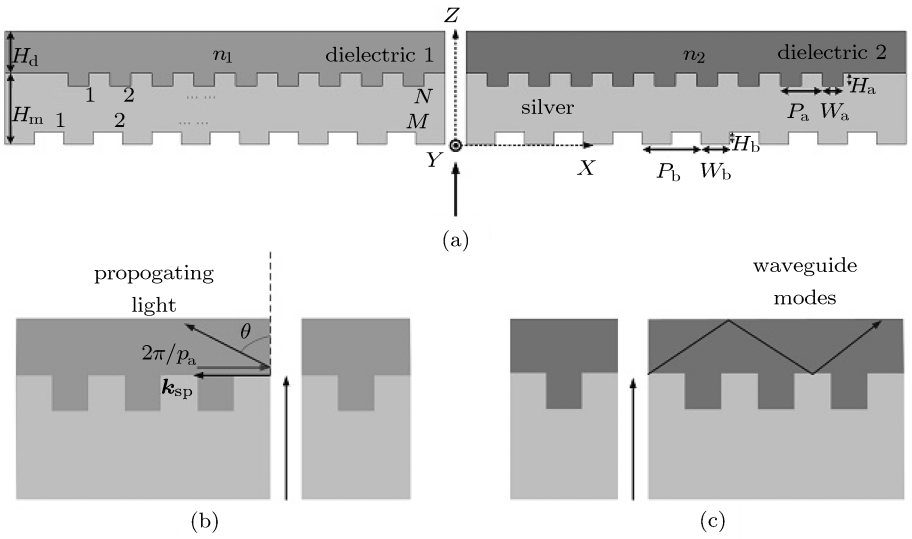


Fig. 1. (a) Schematic diagram of the nanostructure of the proposed metal/dielectric device; (b) definition of the diffraction angle of the propagating light; (c) waveguide modes provided by the dielectric film.

We employ the finite-difference time-domain (FDTD) method to numerically simulate the light transmission through the nanostructure due to its power and intuitiveness. Using the FDTD method, we can observe the field distribution at any time for an arbitrary geometry structure. In the simulation, an incident p-polarized plane wave illuminates the nanostructure in the $+z$ direction from the bottom of the simulation area. Only the p-polarized wave (including E_x, E_z, and H_y) is considered and, consequently, H_x, H_z, and E_y are all zero. The size of the simulation domain is 10 μm × 10 μm, the FDTD grid cell size and time step used in our work are $\Delta x = \Delta z = 10$ nm and $\Delta t = \Delta x/2c$ (c is velocity of light in the vacuum), respectively. The magnetic field intensity $|H_y|^2$ is used to represent the field intensity distribution in our calculation. The perfectly matched layer (PML) boundary condition is used in the x direction and the z direction to absorb the back-reflected radiation as well as the transmitted radiation at the boundaries of the mesh. The FDTD code ran for 6000 time steps in order to produce a steady image. In constructing our device, we chose silver as the film material for its lowest loss in the visible spectrum. The frequency-dependent permittivity of silver is described by the Drude model as

$$\varepsilon_{\rm m}(\omega) = \varepsilon_\infty - \frac{\omega_{\rm p}^2}{\omega^2 + {\rm i}\,\omega\omega_\tau}, \tag{2}$$

where ε_∞ is the infinite frequency dielectric constant, $\omega_{\rm p}$ is the bulk plasma frequency and ω_τ is the collision frequency related to the dissipation loss of the metal. For silver, we choose the dielectric function parameters as follow: $\varepsilon_\infty = 1$, $\omega_{\rm p} = 1.22 \times 10^{16}$ s^{-1}, and $\omega_\tau = 0.9 \times 10^{14}$ s.

3. Results

The simulations of the transmission spectra on different sides of the structure are shown in Fig. 2. From the spectra we know that light beams with different wavelengths can have different intensities at the left and right metal surfaces of the structure. In the 680 nm–780 nm spectral range, the transmission intensity on the left side is larger than that on the right side. In the 950 nm–1050 nm region, the intensity is larger on the right side than on the left side.

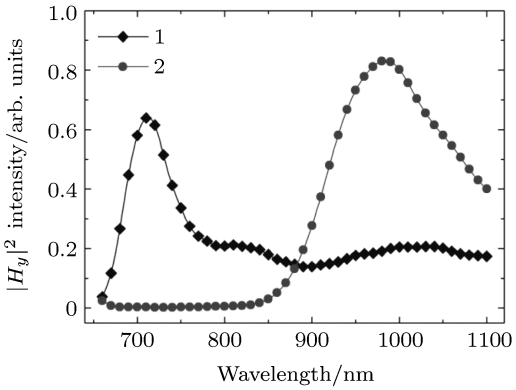


Fig. 2. Spectra of $|H_y|^2$ intensity on different sides. Line 1 represents intensity at the position: 50 nm above the metal surface, and −4 μm on the x axis, and line 2 is for the intensity at 50 nm above the metal surface, 4 μm on the x axis.

To further investigate the proposed structure, we also calculate the x axis dependence intensity of the magnetic field at two specific wavelengths, 760 nm and 1000 nm (shown in Fig. 3). The peak intensity of the left ranges from −4.5 μm to 0 μm is about 100 times that on the right side when the incident light is 760 nm, as shown in Fig. 3(a). The distribution will be opposite if a 1000-nm wave illuminates the structure (see Fig. 3(b)), the peak intensity on the right hand side is still 4∼5 times that on the left-hand side from

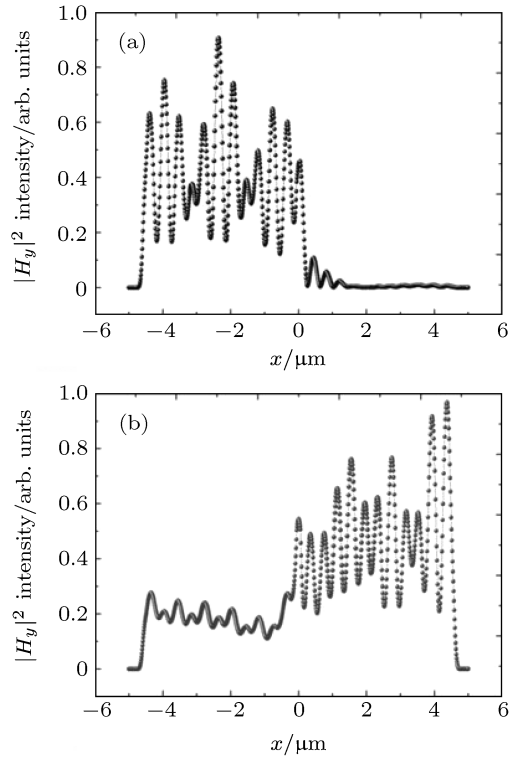


Fig. 3. The $|H_y|^2$ distributions along the x axis 50 nm above the metal surface positions of 760 nm (a) and 1000 nm (b).

0 μm to 4.5 μm. The peaks of the two intensity curves in these graphics each correspond to a groove on the metal surface. It means that the optical intensity in a groove region is extremely larger than that in a top surface region. In other words, the light is trapped in the grooves.

Figures 4(a) and 4(b) show the time-average $|H_y|^2$ distributions of 760-nm and 1000-nm incident light, respectively. As shown in Fig. 4(a), the surface wave is bound to the left corrugated metal/dielectric interface when the incident wavelength is 760 nm. We note that the optical intensity of the right metal surface is weak. In consequence, most of the 760-nm light is guided towards the left side. The 1000-nm wavelength diffraction wave is bounded to the right interface of the metal/dielectric, which is different from the phenomenon of the 760-nm incident wave (see Fig. 4(b)). The intensity on the right-hand side is larger than that on the left-hand side. In other words, the 1000 nm light is guided towards the right-hand side by the metal/dielectric nanostructure.

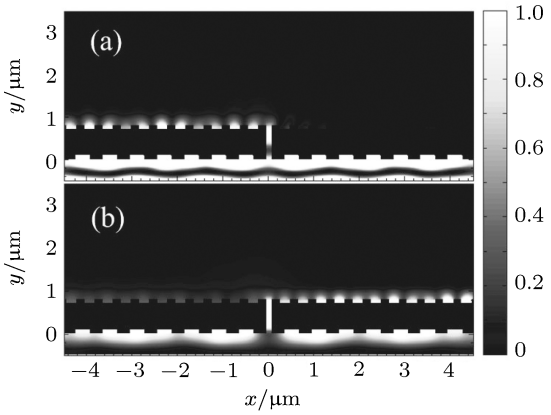


Fig. 4. FDTD simulation results of normalized $|H_y|^2$ distributions for the radiated light positions of 760 nm (a) and 1000 nm (b). A TM-polarized plane wave is incident on the slit from the bottom side in the image.

4. Discussion

Yu *et al.*[22] proposed the physical origin for a directional beam of light emitting from a subwavelength slit in a metallic film characterized by a corrugation feature on the output surface side.[22] The grating equation could also be used to explain the splitting phenomenon

$$k_{\rm sp} \pm m\frac{2\pi}{p_{\rm a}} = k_0 \sin\theta, \tag{3}$$

where $p_{\rm a}$ represents the grating period and θ the diffraction angle. The direction of the propagating light is determined by the difference between the SP wave vector $k_{\rm sp}$ and the grating vector $2\pi/p_{\rm a}$ (Fig. 1(b)). If the SP wave vector $k_{\rm sp}$ and the grating vector $2\pi/p_{\rm a}$ are within a certain range, the direction of the wave will be almost parallel to it and it will propagate along the metal surface ($\theta \to 90°$). In other words, arrays of grooves on the output surface can support surface bound states, which means that the surface wave can be trapped in the metal grating.

Garcia-Vidal *et al.*[23] explored the existence of a surface bound mode in the corrugated surface of a perfect conductor and the dispersion relation of this surface mode can be described as

$$\frac{\sqrt{\boldsymbol{k}_x^2 - \boldsymbol{k}_0^2}}{\boldsymbol{k}_0} = \frac{W_{\rm a}}{P_{\rm a}} \tanh(\boldsymbol{k}_0 H_{\rm a}), \tag{4}$$

where k_x is the component of k_0 in the x direction. The dispersion relation is suitable for explaining the bound states on the surface of our device, as metals are almost perfect conductors from a frequency of zero up to the threshold of the THz regime. If the wave vector matches the surface mode of the periodic structure, the electromagnetic wave will be bounded to the interface. So it is possible to split surface waves of different wavelengths.

In our work, the metallic gratings are designed to have the same parameters but they are covered by an asymmetrical dielectric on both sides. When the incident light transmits though the slit and is diffracted into dielectric films on the two sides, the SP wave vectors $k_{\rm sp}$'s become different because of the different refraction indices of the dielectric adjacent to the metal. From Eq. (1), the SP wave vector $k_{\rm sp}$ is changed when the permittivity of dielectric $\varepsilon_{\rm d}$ is changed. If the changed SP wave vector matches the surface bound modes that the structure supports, the surface wave will be trapped. In the simulation of a 760-nm incident wave, on the left-hand side $k_{\rm sp}$ matches the surface mode and the wave is bounded to the left surface (see Fig. 4(a)). The situation is similar when the incident light is 1000 nm. The difference is the surface wave trap phenomenon occurring in the right interface. The right side $k_{\rm sp}$ matches the surface bound mode, thus the wave is trapped at the right metal/dielectric interface (see Fig. 4(b)). Therefore, the surface wave with a desired wavelength can be split by arranging the output surface grooves and the permittivity of the covered dielectric film.

We know that the dielectric film covering the incoming metallic surface can excite waveguide mode, which drastically enhances the intensity of the transmitted wave.[24,25] In our structure, the dielectric film

covering the output surface can also achieve a similar enhancement of the diffracted surface wave. That is another way to make sure that the diffraction propagates along the surface rather than radiating to the free space. From Fig. 4, we notice that the diffraction wave is well confined in the metal surface and the dielectric film, which is similar to the scenario of light propagating along a dielectric waveguide (Fig. 1(c)). The diffracted light that is enhanced by the waveguide mode can be seen from the dependence of intensity on x in Fig. 3. The peak intensity on the surface does not become weaker when the distance from the central slit increases. The more interesting point is that the intensity of 1000-nm light on the right-hand side turns stronger with x increasing in $+x$ direction (see Fig. 3(b)). We can see that the enhancement of intensity by the waveguide mode is more effective when the incident wavelength is longer. The critical angle for total reflection of the waveguide mode can be calculated from the permittivity of the dielectric and the free space: $\theta_{\rm c} = \arcsin(n_0/n)$. In our device, the critical angles for total reflection of the left and the right dielectric films are 41° and 30°, respectively. For the wavelength of 1000 nm, the diffraction angle θ more easily satisfies the total reflection at the right-hand side dielectric. The diffraction wave will be confined more effectively because of the waveguide modes. That is why the enhancement of intensity by the waveguide mode is more obvious when the incident light wavelength is 1000 nm.

5. Conclusion

We proposed a planar surface wave splitter by covering an asymmetrical dielectric on different sides of a metallic grating structure. It confined and enhanced the emitting light well and may be used in the field of optical chip interconnects or integrated optical circuits due to its valuable characteristics. Adjusting the permittivity of the dielectric on the output leads the counterpart SP wave to be trapped on the surface, which supports the bound condition. We investigated the splitting of the surface wave phenomenon at two specific wavelengths, 760 nm and 1000 nm. The optical intensity of the bounded light at the metal/dielectric interface is [Editor: VALUE MISSING HERE] times that on the unbound side. In other words, the direction of the surface wave, guided by our surface wave splitter, can be determined by its wavelength.

References

[1] Ebbesen T W, Lezec H J, Ghaemi H F, Thio T and Wolff P A 1998 *Nature* **391** 667

[2] Zhang Y, Zhao Q, Liao Z M and Yu D P 2009 *Chin. Phys.* B **18** 4865

[3] Gong Z Q and Liu J Q 2010 *Chin. Phys.* B **19** 067303

[4] Hua Y L, Xin F J, Yan L J, Yuan L Z and Fang Y H 2010 *Chin. Phys.* B **19** 047309

[5] Lezec H J, Degiron A, Devaux E, Linke R A, Martin-Moreno L, Garcia-Vidal F J and Ebbesen T W 2002 *Science* **297** 820

[6] Garcia-Vidal F J, Martin-Moreno L, Lezec H J and Ebbesen T W 2003 *Appl. Phys. Lett.* **83** 4500

[7] Shi H, Du C and Luo X 2007 *Appl. Phys. Lett.* **91** 093111

[8] Wang C, Du C, Lü Y and Luo X 2006 *Opt. Express* **14** 5671

[9] Zhang Y L, Yin Z D, Hong Z C and Ya J X 2008 *Chin. Phys. Lett.* **25** 168

[10] Zhang Y, Zhao D, Zhou C and Jiang X 2009 *J. Appl. Phys.* **105** 113124

[11] Zheng G G and Li X Y 2009 *J. Opt.* A: *Pure Appl. Opt.* **11** 075002

[12] Zheng G G, Shi L X, Wang H L and Li X Y 2009 *Opt. Comm.* **282** 4146

[13] Martín-Moreno L, García-Vidal F J, Lezec H J, Degiron A and Ebbesen T W 2003 *Phys. Rev. Lett.* **90** 167401

[14] Gan Q, Guo B, Song G, Chen L, Fu Z, Ding Y J and Bartoli F J 2007 *Appl. Phys. Lett.* **90** 161130

[15] Caglayan H and Ozbay E 2008 *Opt. Express* **16** 19091

[16] Barnes W L, Dereux A and Ebbesen T W 2003 *Nature* **424** 824

[17] Sambles J R, Bradbery G W and Yang F 1991 *Contemporary Physics* **32** 173

[18] Ritchie R H, Arakawa E T, Cowan J J and Hamm R N 1968 *Phys. Rev. Lett.* **21** 1530

[19] Moreland J, Adams A and Hansma P K 1982 *Phys. Rev.* B **25** 2297

[20] Worthing P T and Barnes W L 2001 *Appl. Phys. Lett.* **79** 3035

[21] García-Vidal F J, Lezec H J, Ebbesen T W and Martín-Moreno L 2003 *Phys. Rev. Lett.* **90** 213901

[22] Yu L B, Lin D Z, Chen Y C, Chang Y C, Huang K T, Liaw J W, Yeh J T, Liu J M, Yeh C S and Lee C K 2005 *Phys. Rev.* B **71** 041405

[23] Garcia-Vidal F J, Martin-Moreno L and Pendry J B 2005 *J. Opt.* A: *Pure Appl. Opt.* **7** S97

[24] Li Z B, Tian J G, Liu Z B, Zhou W Y and Zhang C P 2005 *Opt. Express* **13** 9071

[25] Nikitin A Y, Garcia-Vidal F J and Martin-Moreno L 2009 *J. Opt.* A: *Pure Appl. Opt.* **11** 125702